Supplemental Materials for "Regulation by competition: a hidden layer of gene regulatory network"

Contents

1 A unified coarse-gained competition motif model

Parameters involved in the competition motif model (Fig. 1F) where two target molecule species (target#1 and #2, T_1 and T_2) competitively bind with a shared regulatory molecule species (regulator, R) are described as follows. In general, T_1, T_2 or R is produced with a rate of k_{T1}, k_{T2} or k_R, respectively. Free T_1 (T_1^{F}), T_2 (T_2^{F}) or R (R^{F}) degrades at a rate of g_{T1}, g_{T2} or g_R. T_1^{F} or T_2^{F} binds to R^{F} to form target-regulator complex T_1^{C} or T_2^{C} at a rate of k_{1+} or k_{2+}, and T_1^{C} or T_2^{C} dissociates into R^{F} and T_1^{F} or T_2^{F} at a rate of k_{1-} or k_{2-}. T_1^{C} or T_2^{C} degrades at a rate of g_1 or g_2. Regulators on the complex degrade with the possibility of α_1 or α_2, and targets on the complex degrade with the possibility of β_1 or β_2, thus regulator would recycle from T_1^{C} or T_2^{C} with the possibility of $1-\alpha_1$ or $1-\alpha_2$, target would recycle from T_1^{C} or T_2^{C} with the possibility

of $1-\beta_1$ or $1-\beta_2$, and regulator and target would degrade together with the possibility of $\alpha_1+\beta_1-1$ or $\alpha_2+\beta_2-1$. When R is a repressor, T_1^{F} or T_2^{F} may generate production P_1 or P_2 at a rate of k_{P1} or k_{P2}. In contrast, when R is an activator, T_1^{C} or T_2^{C} may generate production P_1 or P_2 at a rate of k_{P1} or k_{P2}. P_1 or P_2 degrades at a rate of g_{P1} or g_{P2}.

The competing model is described in the following differential equations:

$$\frac{\mathrm{d}\,R^{\mathrm{F}}}{\mathrm{d}\,t} = k_R - g_R R^{\mathrm{F}} - (k_{1+}T_1^{\mathrm{F}} + k_{2+}T_2^{\mathrm{F}})R^{\mathrm{F}} + k_{1-}T_1^{\mathrm{C}} + k_{2-}T_2^{\mathrm{C}} + (1-\alpha_1)g_1T_1^{\mathrm{C}} + (1-\alpha_2)g_2T_2^{\mathrm{C}} \quad (1)$$

$$\frac{\mathrm{d}\,T_1^{\mathrm{F}}}{\mathrm{d}\,t} = k_{T1} - g_{T1}T_1^{\mathrm{F}} - k_{1+}T_1^{\mathrm{F}}R^{\mathrm{F}} + k_{1-}T_1^{\mathrm{C}} + (1-\beta_1)g_1T_1^{\mathrm{C}} \quad (2)$$

$$\frac{\mathrm{d}\,T_1^{\mathrm{C}}}{\mathrm{d}\,t} = k_{1+}T_1^{\mathrm{F}}R^{\mathrm{F}} - k_{1-}T_1^{\mathrm{C}} - g_1T_1^{\mathrm{C}} \quad (3)$$

$$\frac{\mathrm{d}\,T_2^{\mathrm{F}}}{\mathrm{d}\,t} = k_{T2} - g_{T2}T_2^{\mathrm{F}} - k_{2+}T_2^{\mathrm{F}}R^{\mathrm{F}} + k_{2-}T_2^{\mathrm{C}} + (1-\beta_2)g_2T_2^{\mathrm{C}} \quad (4)$$

$$\frac{\mathrm{d}\,T_2^{\mathrm{C}}}{\mathrm{d}\,t} = k_{2+}T_2^{\mathrm{F}}R^{\mathrm{F}} - k_{2-}T_2^{\mathrm{C}} - g_2T_2^{\mathrm{C}} \quad (5)$$

We used this model to describe competitions in various biological processes. In the competition for TF by DNA binding sites (Fig. 1B), T_1 and T_2 represent TF binding sites on DNA and R represents TF. The production and degradation rates of DNA binding sites are set to zero because they are negligible. Complexes degrade with only TF loss ($\alpha \sim 1$, $\beta \sim 0$). When g_1 or g_2 are set to zero, there is no TF loss. For TF as activator, DNA-TF complexes (T_1^{C} and T_2^{C}) can be transcribed into RNA, while for TF as repressor, free DNAs (T_1^{F} and T_2^{F}) can be transcribed (Fig. S1A). In the competition for miRNA by RNA molecules (Fig. 1C), T_1 and T_2 represent two RNA molecule species and R represents miRNA. The loss of miRNA is relatively small so β is set to 1 (Fig. S1B) and as miRNA acts as a repressor, only free RNAs (T_1^{F} and T_2^{F}) translate into proteins. In the case of ribosome allocation (Fig. 1D), where T_1 and T_2 represent two RNA molecule species and R represents ribosome, β is also set to 1 (Fig. S1C). In protein degradation competition (Fig. 1E), where T_1 and T_2 represent two protein molecule species and R represents the protein degradation machine, β is set to 1 too (Fig. S1D). The topology of miRNA-target competition, ribosome-mRNA competition and protein degradation competition are identical except that components generating further production are different.

2 Molecular environment determines shapes of the regulation between competitors

2.1 Solving steady states

Eqs. 1-5 can be solved for steady state when giving all differentials as zero. By adding Eqs. 2 and 3 , we get

$$T_1^{\mathrm{C}} = \frac{k_{T1} - T_1^{\mathrm{F}} g_{T1}}{\beta_1 g_1} \quad (6)$$

By adding Eqs. 1, 3 and 5, we get

$$R^{\mathrm{F}} = \frac{k_R - \alpha_1 T_1^{\mathrm{C}} g_1 - \alpha_2 T_2^{\mathrm{C}} g_2}{g_R} \tag{7}$$

Combining Eqs. 6 and 7, we get

$$R^{\mathrm{F}} = \frac{k_R - \frac{\alpha_1}{\beta_1}(k_{T1} - T_1^{\mathrm{F}} g_{T1}) - \frac{\alpha_2}{\beta_2}(k_{T2} - T_2^{\mathrm{F}} g_{T2})}{g_R} \tag{8}$$

Substituting Eqs. 6 and 8 into Eq. 3, we get

$$(T_1^{\mathrm{F}})^2 - T_1^{\mathrm{F}}(T_1^0 - \lambda_1 - \theta_1 + \phi_{21}) - \lambda_1 T_1^0 = 0 \tag{9}$$

Where

$$T_1^0 = \frac{k_{T1}}{g_{T1}} \qquad T_2^0 = \frac{k_{T2}}{g_{T2}} \tag{10}$$

$$\lambda_1 = \frac{g_R}{\alpha_1 k_{1+}}(\frac{k_{1-}}{g_1} + 1) \qquad \lambda_2 = \frac{g_R}{\alpha_2 k_{2+}}(\frac{k_{2-}}{g_2} + 1) \tag{11}$$

$$\gamma_1 = \frac{\beta_1}{\alpha_1 g_{T1}} \qquad \gamma_2 = \frac{\beta_2}{\alpha_2 g_{T2}} \tag{12}$$

$$\theta_1 = \gamma_1 k_R \qquad \theta_2 = \gamma_2 k_R \tag{13}$$

$$\phi_{21} = \frac{\gamma_1}{\gamma_2}(T_2^0 - T_2^{\mathrm{F}}) \qquad \phi_{12} = \frac{\gamma_2}{\gamma_1}(T_1^0 - T_1^{\mathrm{F}}) \tag{14}$$

Parameters were lumped to represent certain physical meanings to simplify the result. T_i^0 represents the free level of target $\#i$ (T_i) without regulators. $1/\lambda_i$ is proportional to k_{i+}, and negatively correlated with k_{i-}, thus could reflect the strength of binding affinity between T_i and regulator. θ is proportional to k_R, thus could reflect the level of regulator. ϕ_{ji} exhibits the competing regulation effects by target $\#j$ upon to target $\#i$.

Eq. 9 is a quadratic equation of T_1^{F}. Thus, the steady state abundance of free targets can be expressed as

$$T_1^{\mathrm{F}} = \frac{1}{2}(T_1^0 - \lambda_1 - \theta_1 + \phi_{21} + \sqrt{(T_1^0 - \lambda_1 - \theta_1 + \phi_{21})^2 + 4\lambda_1 T_1^0}) \tag{15}$$

$$T_2^{\mathrm{F}} = \frac{1}{2}(T_2^0 - \lambda_2 - \theta_2 + \phi_{12} + \sqrt{(T_2^0 - \lambda_2 - \theta_2 + \phi_{12})^2 + 4\lambda_2 T_2^0}) \tag{16}$$

2.2 Explanations on regimes and related phenomena

Assuming that the binding between targets and regulator is very strong, λ_i becomes negligible, thus Eq. 15 can be simplified as follows:

$$T_1^{\mathrm{F}} \simeq \begin{cases} \dfrac{\lambda_1 T_1^0}{\theta_1 - T_1^0 - \frac{\gamma_1}{\gamma_2}(T_2^0 - T_2^{\mathrm{F}})} \simeq 0 & \text{, if } T_1^0 + \phi_{21} < \theta_1 \\ T_1^0 - \theta_1 + \dfrac{\gamma_1}{\gamma_2}(T_2^0 - T_2^{\mathrm{F}}) & \text{, if } T_1^0 + \phi_{21} > \theta_1 \end{cases} \tag{17}$$

Meanwhile, the steady-state abundance of T_1^{C} and T_2^{C} can be calculated from Eq. 6:

$$T_1^{\mathrm{C}} = \frac{g_{T1}}{\beta_1 g_1}(T_1^0 - T_1^{\mathrm{F}}) \qquad\qquad T_2^{\mathrm{C}} = \frac{g_{T2}}{\beta_2 g_2}(T_2^0 - T_2^{\mathrm{F}}) \tag{18}$$

and can be simplified using Eq. 17:

$$T_1^{\mathrm{C}} \simeq \begin{cases} \dfrac{g_{T1}}{g_1\beta_1} T_1^0 & \text{, if } T_1^0 + \phi_{21} < \theta_1 \\ \dfrac{g_{T1}}{g_1\beta_1}(\theta_1 - \dfrac{\alpha_2 g_2 \beta_1}{\alpha_1 g_{T1}} T_2^{\mathrm{C}}) & \text{, if } T_1^0 + \phi_{21} > \theta_1 \end{cases} \tag{19}$$

The turning point in Eqs. 17 and 19:

$$T_1^0 + \phi_{21} = \theta_1 \tag{20}$$

can be regarded as a threshold to distinguish regimes of the system: "R abundant" ($T_1^0 + \phi_{21} \ll \theta_1$), "$R$ equimolar" ($T_1^0 + \phi_{21} \simeq \theta_1$) and "$R$ scarce" ($T_1^0 + \phi_{21} \gg \theta_1$). Eqs. 17 and 19 explain why the relationships between competitors are piecewise (Fig. 2A-C). For T_1^{F} and T_2^{F}, according to Eq. 17, in "R abundant" regime ($T_1^0 + \phi_{21} \ll \theta_1$), almost all targets bind with R, so the level of T_1^{F} approaches to zero. In the contrary, in "R scarce" regime ($T_1^0 + \phi_{21} \gg \theta_1$), T_1^{F} increases with the increment of T_2^{F}, which is because when the production rate of T_2 raises to sequester R, T_2^{C} increases thus $T_2^0 - T_2^{\mathrm{F}}$ increases according to Eq. 18. Given the above, when the production rate of T_2 increases to switch the system from R "abundant" regime to "R scarce" regime, the abundance of T_1^{F} will exhibit a "threshold behavior" (Fig. 2B).

Similarly, Eq. 19 suggested that the relationship between T_1^{C} and T_2^{C} is piecewise linear. If R is abundant ($T_1^0 + \phi_{21} \ll \theta_1$), T_1^{C} would keep substantially unchanged, while when R is scarce ($T_1^0 + \phi_{21} \gg \theta_1$), T_1^{C} would decrease linearly with the increment of T_2^{C}, thus shows "negative linear dependence" (Fig. 2C).

2.3 Approximation of the regime threshold

The threshold (Eq. 20) can be approximated based on the strong binding assumption. It is equivalent to:

$$\frac{k_{T1}}{g_{T1}} + \frac{\alpha_2\beta_1 g_{T2}}{\alpha_1\beta_2 g_{T1}}(\frac{k_{T2}}{g_{T2}} - T_2^{\mathrm{F}}) = \frac{\beta_1 k_R}{\alpha_1 g_{T1}} \tag{21}$$

From Eq. 3, we get

$$T_1^{\mathrm{F}} = \frac{k_{1-} + g_1}{R^{\mathrm{F}} k_{1+}} T_1^{\mathrm{C}} \tag{22}$$

According to Eq. 17, before the system reaches the threshold ($T_1^0 + \phi_{21} \leq \theta_1$) in the process of increment of production of T_2, T_1^{F} is much smaller than T_1^{C} and approaches to zero, and so does T_2^{F}. Thus, the threshold point ($T_1^0 + \phi_{21} = \theta_1$) could be approximated from Eq. 21 as:

$$\frac{\alpha_1}{\beta_1} k_{T1} + \frac{\alpha_2}{\beta_2} k_{T2} = k_R \tag{23}$$

Eq. 23 gives an approximation of the threshold position to estimate the regime of a competing system roughly.

3 Competition can shape the regulator-target response curve

3.1 How competition shapes regulator-target response curve

According to Eq. 9, there are

$$F(k_R, T_1^{\mathrm{F}}, T_2^{\mathrm{F}}) = (T_1^{\mathrm{F}})^2 - T_1^{\mathrm{F}}(T_1^0 - \lambda_1 - \theta_1 + \phi_{21}) - \lambda_1 T_1^0 = 0 \tag{24}$$

$$G(k_R, T_1^{\mathrm{F}}, T_2^{\mathrm{F}}) = (T_2^{\mathrm{F}})^2 - T_2^{\mathrm{F}}(T_2^0 - \lambda_2 - \theta_2 + \phi_{12}) - \lambda_2 T_2^0 = 0 \tag{25}$$

Thus,

$$\frac{\partial T_1^{\mathrm{F}}}{\partial k_R} = \frac{\begin{vmatrix} \frac{\partial F}{\partial k_R} & \frac{\partial F}{\partial T_2^{\mathrm{F}}} \\ \frac{\partial G}{\partial k_R} & \frac{\partial G}{\partial T_2^{\mathrm{F}}} \end{vmatrix}}{\begin{vmatrix} \frac{\partial F}{\partial T_1^{\mathrm{F}}} & \frac{\partial F}{\partial T_2^{\mathrm{F}}} \\ \frac{\partial G}{\partial T_1^{\mathrm{F}}} & \frac{\partial G}{\partial T_2^{\mathrm{F}}} \end{vmatrix}} = -\frac{\gamma_1}{1 + \frac{\lambda_1 T_1^0}{\lambda_2 T_2^0}(\frac{T_2^{\mathrm{F}}}{T_1^{\mathrm{F}}})^2 + \frac{\lambda_1 T_1^0}{(T_1^{\mathrm{F}})^2}} \tag{26}$$

$$\frac{\partial \log T_1^{\mathrm{F}}}{\partial \log k_R} = \frac{k_R}{T_1^{\mathrm{F}}}\frac{\partial T_1^{\mathrm{F}}}{\partial k_R} = -\frac{\gamma_1 k_R}{T_1^{\mathrm{F}} + \frac{\lambda_1 T_1^0}{\lambda_2 T_2^0}\frac{(T_2^{\mathrm{F}})^2}{T_1^{\mathrm{F}}} + \frac{\lambda_1 T_1^0}{T_1^{\mathrm{F}}}} \tag{27}$$

Eq. 27 describes the derivative of regulator-target response curve (Fig. 2E and 2G).

Similarly, the buffer capacity, which quantifies the ability to resist pH changes in buffer solution, can be calculated as

$$B = -\frac{\partial k_R}{\partial \log T_1^{\mathrm{F}}} = \frac{1}{\gamma_1}(T_1^{\mathrm{F}} + \frac{\lambda_1 T_1^0}{\lambda_2 T_2^0}\frac{(T_2^{\mathrm{F}})^2}{T_1^{\mathrm{F}}} + \frac{\lambda_1 T_1^0}{T_1^{\mathrm{F}}}) \tag{28}$$

3.2 Competition in buffer solution

For any buffer solution with a weak acid (HA) and its conjugate base (A^-) or a weak base (BOH) and its conjugate acid (B^+), there are

$$H_2O \rightleftharpoons H^+ + OH^-$$

$$HA \rightleftharpoons H^+ + A^-$$

$$BOH \rightleftharpoons B^+ + OH^-$$

Here we take ammonium buffer solution ($NH_3 \cdot H_2O$ and NH_4Cl) as an example. In a aqueous solution with a mol/L $NH_3 \cdot H_2O$ and b mol/L NH_4Cl, there are

$$H_2O \rightleftharpoons H^+ + OH^-$$

$$NH_3 \cdot H_2O \rightleftharpoons {NH_4}^+ + OH^-$$

The equilibrium constants of these two reactions are

$$K_1 = \frac{[H^+][OH^-]}{[H_2O]} \tag{29}$$

$$K_2 = \frac{[{NH_4}^+][OH^-]}{[NH_3 \cdot H_2O]} \tag{30}$$

Because the concertation water of in an aqueous solution is almost invariant, the equilibrium constant of water (ion-product constant) is defined as

$$K_{\mathrm{w}} = [\mathrm{H}^+][\mathrm{OH}^-] = K_1[\mathrm{H_2O}] \simeq 10^{-14}\,\mathrm{mol}\cdot\mathrm{L}$$

Here, we consider H^+ (T_1) and $\mathrm{NH_4}^+$ (T_2) competing for OH^- (R). Thus, Eqs. 29 and 30 is equivalent to

$$K_1 = \frac{T_1^{\mathrm{F}} R^{\mathrm{F}}}{T_1^{\mathrm{C}}} \tag{31}$$

$$K_2 = \frac{T_2^{\mathrm{F}} R^{\mathrm{F}}}{T_2^{\mathrm{C}}} \tag{32}$$

Meanwhile, because there are no production and degradation of any component, every substance is conserved as

$$T_1^{\mathrm{F}} + T_1^{\mathrm{C}} = T_1^{\mathrm{A}} = w \tag{33}$$

$$T_2^{\mathrm{F}} + T_2^{\mathrm{C}} = T_2^{\mathrm{A}} = a + b \tag{34}$$

$$T_1^{\mathrm{C}} + T_2^{\mathrm{C}} + R^{\mathrm{F}} = R^{\mathrm{A}} = a + w \tag{35}$$

Combining Eqs. 33-35, we get

$$R^{\mathrm{F}} = R^{\mathrm{A}} - T_1^{\mathrm{A}} - T_2^{\mathrm{A}} + T_1^{\mathrm{F}} + T_2^{\mathrm{F}} \tag{36}$$

Combining Eqs. 31, 32 and 36, we get

$$T_1^{\mathrm{F}} = \frac{1}{2}(T_1^{\mathrm{A}} + T_2^{\mathrm{A}} - R^{\mathrm{A}} - T_2^{\mathrm{F}} - K_1 + \sqrt{(T_1^{\mathrm{A}} + T_2^{\mathrm{A}} - R^{\mathrm{A}} - T_2^{\mathrm{F}} - K_1)^2 + 4K_1T_1^0}) \tag{37}$$

which is a degenerate form of Eq. 15, where

$$\alpha_1 = \alpha_2 = \beta_1 = \beta_2 \qquad g_{T1} = g_{T2}$$

$$K_1 = \frac{g_R}{\alpha_1 k_{1+}}(\frac{k_{1-}}{g_1} + 1) \qquad K_2 = \frac{g_R}{\alpha_2 k_{2+}}(\frac{k_{2-}}{g_2} + 1)$$

$$T_1^{\mathrm{A}} = k_{T1}/g_{T1} \qquad T_2^{\mathrm{A}} = k_{T2}/g_{T2}$$

$$R^{\mathrm{A}} = k_R/g_{T1} = k_R/g_{T2}$$

According to Eq. 28, the buffer capacity of this solution is

$$B = \frac{\partial R}{\partial \mathrm{pOH}} = T_1^{\mathrm{F}} + \frac{K_{\mathrm{w}}}{K_2 T_2^{\mathrm{A}}}\frac{(T_2^{\mathrm{F}})^2}{T_1^{\mathrm{F}}} + \frac{K_{\mathrm{w}}}{T_1^{\mathrm{F}}} = [\mathrm{OH}^-] + \frac{K_2(a+b)[\mathrm{OH}^-]}{(K_2 + [\mathrm{OH}^-])^2} + [\mathrm{H}^+] \tag{38}$$

Eq. 38 indicates that when a mild change of OH^- is introduced to the solution, the buffer capacity guarantees the stable of pOH (and pH). More buffer substance ($\mathrm{NH_4}^+$ and $\mathrm{NH_3}\cdot\mathrm{H_2O}$, $a+b$) can lead to a larger buffer capacity, and the buffer capacity may maximize when $\mathrm{pH} = \mathrm{p}K_2$.

3.3 Dose-response curve of free target to free regulator

Substituting Eq. 22 into Eq. 2, we get

$$k_{T1} - T_1^{\mathrm{F}} g_{T1} - k_{1+} R^{\mathrm{F}} T_1^{\mathrm{F}} + (k_{1-} + (1-\beta_1) g_1) T_1^{\mathrm{C}} = 0 \tag{39}$$

Thus,

$$\frac{T_1^{\mathrm{F}}}{T_1^0} = \frac{1}{1 + O_1 R^{\mathrm{F}}}, \text{ where } O_1 = \frac{\beta_1 k_{1+}}{g_{T1}(1 + \frac{k_{1-}}{g_1})} \tag{40}$$

In system with n targets competing for same regulator, for the ith target ($i = 1,\ 2,\ \cdots,\ n$), this result can be extended as:

$$\frac{T_i^{\mathrm{F}}}{T_i^0} = \frac{1}{1 + O_i R^{\mathrm{F}}}, \text{ where } O_i = \frac{\beta_i k_{i+}}{g_{Ti}(1 + \frac{k_{i-}}{g_i})} \tag{41}$$

Similarly,

$$\frac{T_i^{\mathrm{C}}}{T_i^0} = \frac{g_{Ti}}{\beta_i g_i}(1 - \frac{1}{1 + O_i R^{\mathrm{F}}}) \tag{42}$$

Eqs. 41 and 42 indicate that the level of T_i^{F} and T_i^{C} are determined only by the free level of R, and some chemical kinetic parameters of T_i and R. In another words if two or more tagets compete for shared R, the relative abundances of each free target or complex are independent of other targets when giving the free level of R. In the siRNA design strategy [1, 2], this property guarantees that no matter what expression of the off-target gene is (unless the expression is zero), the amount of free siRNA required to repress the target gene to a certain extent would always repress the off-target gene to a certain extent, which is determined by O_{on} and O_{off}, as described in Eq. 41. When giving the expression of any target gene, siRNA could act as a medium to predict the expression of other target genes. This property also guides how to select suitable chemical reaction parameters: a good siRNA should have large O_{on} and small O_{off}.

4 Competition can delay or accelerate dynamic response

When R level changes, comparisons of $\frac{\mathrm{d}\, R^{\mathrm{F}}}{\mathrm{d}\, t}$ tells how competition affects the dynamic response speed of T_1 with respect to R. According to Eq. 1 and 5,

$$\begin{aligned} \frac{\mathrm{d}\, R^{\mathrm{F}}}{\mathrm{d}\, t} =& k_R - g_R R^{\mathrm{F}} - k_{1+} T_1^{\mathrm{F}} R^{\mathrm{F}} + k_{1-} T_1^{\mathrm{C}} + (1-\alpha_1) g_1 T_1^{\mathrm{C}} \\ & \underbrace{-k_{2+} T_2^{\mathrm{F}} R^{\mathrm{F}} + k_{2-} T_2^{\mathrm{C}} + g_2 T_2^{\mathrm{C}}}_{\mathrm{A}}\ \underbrace{-\alpha_2 g_2 T_2^{\mathrm{C}}}_{\mathrm{B}} \end{aligned} \tag{43}$$

Item A equals to $-\frac{\mathrm{d}\, T_2^{\mathrm{C}}}{\mathrm{d}\, t}$, and indicates the ability of T_2 to sequester R when T_2^{C} forms ($-\frac{\mathrm{d}\, T_2^{\mathrm{C}}}{\mathrm{d}\, t} < 0$), or release R when T_2^{C} dissociates ($-\frac{\mathrm{d}\, T_2^{\mathrm{C}}}{\mathrm{d}\, t} > 0$). Item B indicates the level of R loss mediated by T_2^{C} degradation.

On the rising edge of R, T_2^{C} forms so item A < 0, meanwhile item B < 0 all the time, thus $\frac{\mathrm{d}\, R^{\mathrm{F}}}{\mathrm{d}\, t}$ is smaller than non-competing system, leading to a slower response. On the falling edge of R, item A > 0 while item B < 0, thus the response speed depends on the relative magnitude of item A and B. As g_2 or α_2 increases, the absolute value of item B increases to alter the response from delay to acceleration. As k_2^+ increases or

k_2^- decreases, item A increases while the absolute value of item B also increases because T_2^{C} becomes larger, thus delay the response when there is no R loss mediated by T_2^{C} ($g_2 = 0$, Fig. S3D), alter the response from delay to acceleration when g_2 is moderate (Fig. S3E), or accelerate the response when g_2 is large enough (Fig. S3F).

5 Noise and correlated flucuation evaluation

The variances and co-variances of the molecular species in the system can be estimated with linear noise approximation [3]. Fluctuation-dissipation theorem provides a general way to quantifies the fluctuations. The fluctuation-dissipation equation was solved numerically to calculate the covariance matrix $\boldsymbol{C}$, the diagonal elements of which are the variance of corresponding entities, while the off-diagonal elements of which describe the co-variances between molecular species. The noise of a molecular species i is defined as coefficient of variation $\sigma(x_i)/\bar{x}_i$ and the correlation between two molecular species i and j is defined as $\mathrm{cov}(x,y)/(\sigma(x_i)\sigma(x_j))$, where x_i and x_j are random variables representing the abundance of molecular species i and j.

Taking miRNA competing system as an example (where miRNA acts as repressor), the vector of molecular number

$$\boldsymbol{N} = \begin{bmatrix} R^{\mathrm{F}} & T_1^{\mathrm{F}} & T_2^{\mathrm{F}} & T_1^{\mathrm{C}} & T_2^{\mathrm{C}} & P_1 & P_2 \end{bmatrix} \tag{44}$$

Transition rates vector is

$$\begin{aligned} \boldsymbol{f}(\boldsymbol{x}) = \Big[\quad & k_{T1} \quad g_{T1}T_1^{\mathrm{F}} \quad k_{1+}T_1^{\mathrm{F}}R^{\mathrm{F}} \quad k_{1-}T_1^{\mathrm{C}} \quad g_1(1-\beta_1)T_1^{\mathrm{C}} \quad k_{T2} \quad g_{T2}T_2^{\mathrm{F}} \\ & k_{2+}T_2^{\mathrm{F}}R^{\mathrm{F}} \quad k_{2-}T_2^{\mathrm{C}} \quad g_2(1-\beta_2)T_2^{\mathrm{C}} \quad k_R \quad g_R R^{\mathrm{F}} \quad g_1(1-\alpha_1)T_1^{\mathrm{C}} \\ & g_1(\alpha_1+\beta_1-1)T_1^{\mathrm{C}} \quad g_2(1-\alpha_2)T_2^{\mathrm{C}} \quad g_2(\alpha_2+\beta_2-1)T_2^{\mathrm{C}} \quad k_{P1}T_1^{\mathrm{F}} \\ & g_{P1}P_1 \quad k_{P2}T_2^{\mathrm{F}} \quad g_{P2}P_2 \Big] \end{aligned} \tag{45}$$

Stoichiometric matrix is

$$\boldsymbol{S} = \begin{bmatrix} 1 & -1 & -1 & 1 & 1 & 0 & 0 & 0 & 0 & 0 & 0 & 0 & 0 & 0 & 0 & 0 & 0 & 0 & 0 & 0 \\ 0 & 0 & 0 & 0 & 0 & 1 & -1 & -1 & 1 & 1 & 0 & 0 & 0 & 0 & 0 & 0 & 0 & 0 & 0 & 0 \\ 0 & 0 & -1 & 1 & 0 & 0 & 0 & -1 & 1 & 0 & 1 & -1 & 1 & 1 & 0 & 0 & 0 & 0 & 0 & 0 \\ 0 & 0 & 1 & -1 & -1 & 0 & 0 & 0 & 0 & 0 & 0 & 0 & -1 & 0 & -1 & 0 & 0 & 0 & 0 & 0 \\ 0 & 0 & 0 & 0 & 0 & 0 & 0 & 1 & -1 & -1 & 0 & 0 & 0 & -1 & 0 & -1 & 0 & 0 & 0 & 0 \\ 0 & 0 & 0 & 0 & 0 & 0 & 0 & 0 & 0 & 0 & 0 & 0 & 0 & 0 & 0 & 0 & 1 & -1 & 0 & 0 \\ 0 & 0 & 0 & 0 & 0 & 0 & 0 & 0 & 0 & 0 & 0 & 0 & 0 & 0 & 0 & 0 & 0 & 0 & 1 & -1 \end{bmatrix} \tag{46}$$

In the steady state, the rate equations can be linearized by the Jacobian matrix:

$$\boldsymbol{J} = \boldsymbol{S} \cdot \frac{\partial \boldsymbol{f}(\boldsymbol{x})}{\partial \boldsymbol{N}} \tag{47}$$

The diffusion matrix $\boldsymbol{D}$ is

$$\boldsymbol{D} = \boldsymbol{S} \cdot \mathrm{diag}\left(\boldsymbol{f}(\boldsymbol{x})\right) \cdot \boldsymbol{S}^{\top} \tag{48}$$

Therefore, the covariance matrix $\boldsymbol{C}$ can be calculate numerically by solving the fluctuation dissipation equation:

$$\boldsymbol{J}\cdot\boldsymbol{C}+\boldsymbol{C}\cdot\boldsymbol{J}^{\top}+\boldsymbol{D}=\boldsymbol{0} \tag{49}$$

6 Regulator allocation to multiple targets

When there are n targets, similarly to Eqs. 1-5, there are

$$\frac{\mathrm{d}\,R^{\mathrm{F}}}{\mathrm{d}\,t}=k_R-g_R R^{\mathrm{F}}+\sum_{i=1}^{n}(-k_{i+}T_i^{\mathrm{F}}R^{\mathrm{F}}+k_{i-}T_i^{\mathrm{C}}+(1-\alpha_i)g_iT_i^{\mathrm{C}}) \tag{50}$$

$$\frac{\mathrm{d}\,T_i^{\mathrm{F}}}{\mathrm{d}\,t}=k_{Ti}-g_{Ti}T_i^{\mathrm{F}}-k_{i+}T_i^{\mathrm{F}}R^{\mathrm{F}}+k_{i-}T_i^{\mathrm{C}}+(1-\beta_i)g_iT_i^{\mathrm{C}} \tag{51}$$

$$\frac{\mathrm{d}\,T_i^{\mathrm{C}}}{\mathrm{d}\,t}=k_{i+}T_i^{\mathrm{F}}R^{\mathrm{F}}-k_{i-}T_i^{\mathrm{C}}-g_iT_i^{\mathrm{C}} \tag{52}$$

At steady states, by adding Eqs. 50 and 52, we get

$$R^{\mathrm{F}}=\frac{k_R-\sum_i\alpha_iT_i^{\mathrm{C}}g_i}{g_R} \tag{53}$$

Solving Eq. 52, we get

$$T_i^{\mathrm{F}}=\frac{k_{i-}+g_i}{R^{\mathrm{F}}k_{i+}}T_i^{\mathrm{C}} \tag{54}$$

Combining Eqs. 53 and 54, we get

$$R^{\mathrm{F}}=\frac{k_R}{g_R+\sum_i Q_i} \tag{55}$$

where

$$Q_i=\alpha_ig_i\frac{k_{i+}}{k_{i-}+g_i}T_i^{\mathrm{F}} \tag{56}$$

Thus,

$$\alpha_ig_iT_i^{\mathrm{C}}=\frac{Q_i}{g_R+\sum_j Q_j}k_R \tag{57}$$

Eq. 57 has the exact form of current divider rule in electronics:

$$I_i=\frac{\frac{1}{R_i}}{\frac{1}{R_0}+\sum_j\frac{1}{R_j}}I_{\mathrm{total}} \tag{58}$$

It inspires that R's production rate (k_R) is analogous to the total current (I_{total}); the capability of T_i^{C} to consume R ($\alpha_ig_iT_i^{C}$) is analogous to the ith branch current (I_i); and the capability of T_i^{F} to occupy R (Q_i) is analogous to the ith branch conductance ($1/R_i$).

When R is scarce, $T_i^{\mathrm{F}}\simeq T_i^0$, thus Eq. 56 is approximated to

$$Q_i\simeq\alpha_ig_i\frac{k_{i+}}{k_{i-}+g_i}T_i^0 \tag{59}$$

which indicates that in the "R scarce" regime, the capability of T_i to occupy R (resistance) is only determined by the parameter settings of T_i.

For catalytic reactions with a constat level of enzyme (regulator) and substances (targets), Eqs. 50-52 degenerate as

$$\frac{\mathrm{d}\,R^{\mathrm{F}}}{\mathrm{d}\,t} = \sum_{i=1}^{n}(-k_{i+}T_i^{\mathrm{F}}R^{\mathrm{F}} + k_{i-}T_i^{\mathrm{C}} + g_iT_i^{\mathrm{C}}) \tag{60}$$

$$\frac{\mathrm{d}\,T_i^{\mathrm{F}}}{\mathrm{d}\,t} = -k_{i+}T_i^{\mathrm{F}}R^{\mathrm{F}} + k_{i-}T_i^{\mathrm{C}} \tag{61}$$

$$\frac{\mathrm{d}\,T_i^{\mathrm{C}}}{\mathrm{d}\,t} = k_{i+}T_i^{\mathrm{F}}R^{\mathrm{F}} - k_{i-}T_i^{\mathrm{C}} - g_iT_i^{\mathrm{C}} \tag{62}$$

Under the assumption of Michaelis-Menten kinetics that $\frac{\mathrm{d}\,T_i^{\mathrm{C}}}{\mathrm{d}\,t} = 0$, define $K_i = (k_{i-} + g_i)/k_{i+}$, then we get

$$T_i^{\mathrm{C}} = \frac{T_i^{\mathrm{F}}}{K_i}R^{\mathrm{F}} \tag{63}$$

Thus,

$$R^{\mathrm{total}} = R^{\mathrm{F}} + \sum_j T_j^{\mathrm{C}} = R^{\mathrm{F}}(1 + \sum_j T_j^{\mathrm{F}}/K_j) \tag{64}$$

$$R^{\mathrm{F}} = \frac{1}{1 + \sum_j T_i^{\mathrm{F}}/K_i}R^{\mathrm{total}} \tag{65}$$

$$T_i^{\mathrm{C}} = \frac{T_i^{\mathrm{F}}/K_i}{1 + \sum_j T_j^{\mathrm{F}}/K_j}R^{\mathrm{total}} \tag{66}$$

Which is the formation of enzyme allocation in Michaelis-Menten kinetics systems [4].

7 Simulation parameters for drawing figures

The scales of simulation parameters are referenced from previous publications across different competition scenarios, such as transcription [5], post-transcription [6, 7],translation [8],degradation [9]and chemical buffer solutions. Table S1 lists the parameters for drawing figures, the scales of which are derived from from previous researches on ceRNA effects [1, 2, 6]. All gradually changing parameters are shown in figures. In Fig. 2F-G and S2D-E, $k_{T2} = 1 \times 10^{-2}$. In Fig. 2I, $k_{T2} = 1 \times 10^{-4}$, and parameters of T_3 are shown in Table S1. In Fig. 3A-C and S3A-F, $g_1 = 4 \times 10^{-5}$, $k_{T2} = 1 \times 10^{-4}$. In Fig. S3A, $g_2 = 3.2 \times 10^{-4}$. In Fig. 3E-H, for dashed blue lines, $k_R = 5 \times 10^{-3}$; for thick blue lines, $k_R = 7.81 \times 10^{-5}$; for thick green lines, $k_R = 5 \times 10^{-3}$, $k_{T2} = 3.21 \times 10^{-2}$. In Fig. S3G-J, $k_{T1} = 5 \times 10^{-3}$.

References

[1] Yuan Y, Liu B, Xie P, Zhang MQ, Li Y, Xie Z, et al. Model-guided quantitative analysis of microRNA-mediated regulation on competing endogenous RNAs using a synthetic gene circuit. Proceedings of the National Academy of Sciences. 2015;112(10):3158–3163.

[2] Yuan Y, Ren X, Xie Z, Wang X. A quantitative understanding of microRNA-mediated competing endogenous RNA regulation. Quantitative Biology. 2016;4(1):47–57.

[3] Elf J, Ehrenberg M. Fast evaluation of fluctuations in biochemical networks with the linear noise approximation. Genome research. 2003;13(11):2475–2484.

[4] Chou TC, Talaly P. A simple generalized equation for the analysis of multiple inhibitions of Michaelis-Menten kinetic systems. Journal of Biological Chemistry. 1977;252(18):6438–6442.

[5] Jayanthi S, Nilgiriwala KS, Del Vecchio D. Retroactivity controls the temporal dynamics of gene transcription. ACS synthetic biology. 2013;2(8):431–441.

[6] Ala U, Karreth FA, Bosia C, Pagnani A, Taulli R, Léopold V, et al. Integrated transcriptional and competitive endogenous RNA networks are cross-regulated in permissive molecular environments. Proceedings of the National Academy of Sciences. 2013;110(18):7154–7159.

[7] Schmiedel JM, Klemm SL, Zheng Y, Sahay A, Blüthgen N, Marks DS, et al. MicroRNA control of protein expression noise. Science. 2015;348(6230):128–132.

[8] Gorochowski TE, Avcilar-Kucukgoze I, Bovenberg RA, Roubos JA, Ignatova Z. A minimal model of ribosome allocation dynamics captures trade-offs in expression between endogenous and synthetic genes. ACS synthetic biology. 2016;5(7):710–720.

[9] Cookson NA, Mather WH, Danino T, Mondragón-Palomino O, Williams RJ, Tsimring LS, et al. Queueing up for enzymatic processing: correlated signaling through coupled degradation. Molecular systems biology. 2011;7(1):561.

Table S1 Primary parameters for simulations

Primary parameters						Additional parameters for Fig. 2I	
R		T_1		T_2		T_3	
k_R	5×10^{-3}	k_{T1}	1×10^{-3}	k_{T2}	8×10^{-3}	k_{T3}	5×10^{-4}
g_R	1×10^{-4}	g_{T1}	1×10^{-5}	g_{T2}	1×10^{-5}	g_{T3}	1×10^{-5}
		k_{1+}	1×10^{-4}	k_{2+}	1×10^{-4}	k_{3+}	1×10^{-6}
		k_{1-}	5×10^{-5}	k_{2-}	5×10^{-5}	k_{3-}	5×10^{-5}
		g_1	8×10^{-5}	g_2	8×10^{-5}	g_3	1×10^{-5}
		α_1	1	α_2	0.5	α_3	0.5
		β_1	1	β_2	1	β_3	1
		k_{P1}	1×10^{-2}				
		g_{P1}	5×10^{-6}				

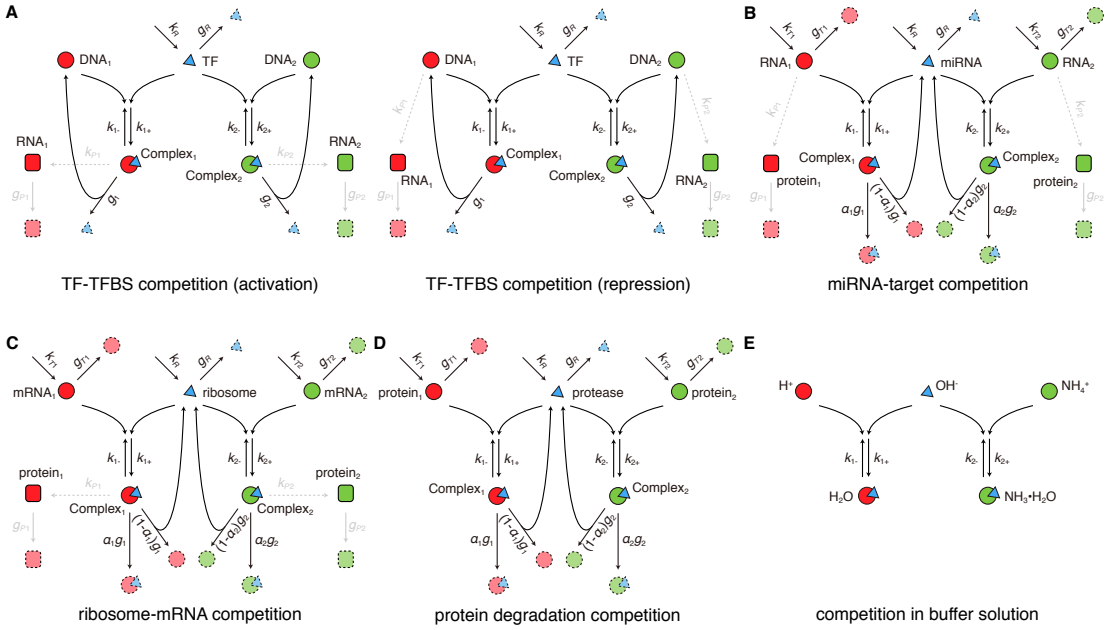

Figure S1 Detailed descriptions under the unified coarse-gained competition motif model for diverse competition scenarios.

(*A*) DNA TF binding sites (TFBS) competing for TFs. Left: TF acts as an activator; right: TF acts as a repressor.

(*B*) RNA molecules competing for miRNAs.

(*C*) RNA molecules competing for ribosomes.

(*D*) Proteins competing for proteases.

(*E*) Competition in the ammonium buffer solution, where H^+ and NH_4^+ compete for OH^-.

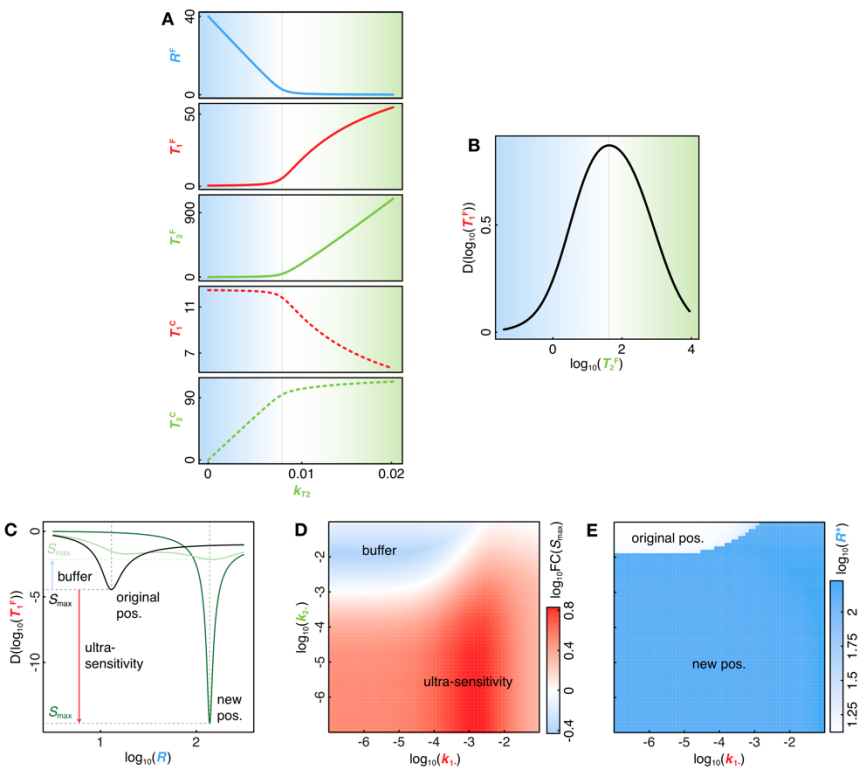

Figure S2 Steady state behaviors of competition systems.

(*A*) Abundances of each component in Figure 2A on linear scales.

(*B*) Derivatives of the curve in Figure 2B. Each component's abundance in competition motif changing with T_2's production rate (k_{T2}). Colors, lines and parameter settings are the same with Figure 2A-C.

(*C*) Schematic diagram depicting the maximum sensitivity (S_{max}) and its position (R^*) of R-T_1 dose-response curves. Dose-response curves are adopted from Figure 3G.

(*D-E*) Relative binding affinities of T_1 and T_2 ($k_{1\text{-}}$ and $k_{2\text{-}}$) shape R-T_1 dose-response curves. (*D*) Fold change of S_{max} compared with that of non-competing system (k_{T2}=0). Competition of T_2 buffers the response of T_1^F to R when $\log_{10}FC(S_{max})<0$, but introduces larger sensitivity when $\log_{10}FC(S_{max})>0$. (*E*) Changes of R^*.

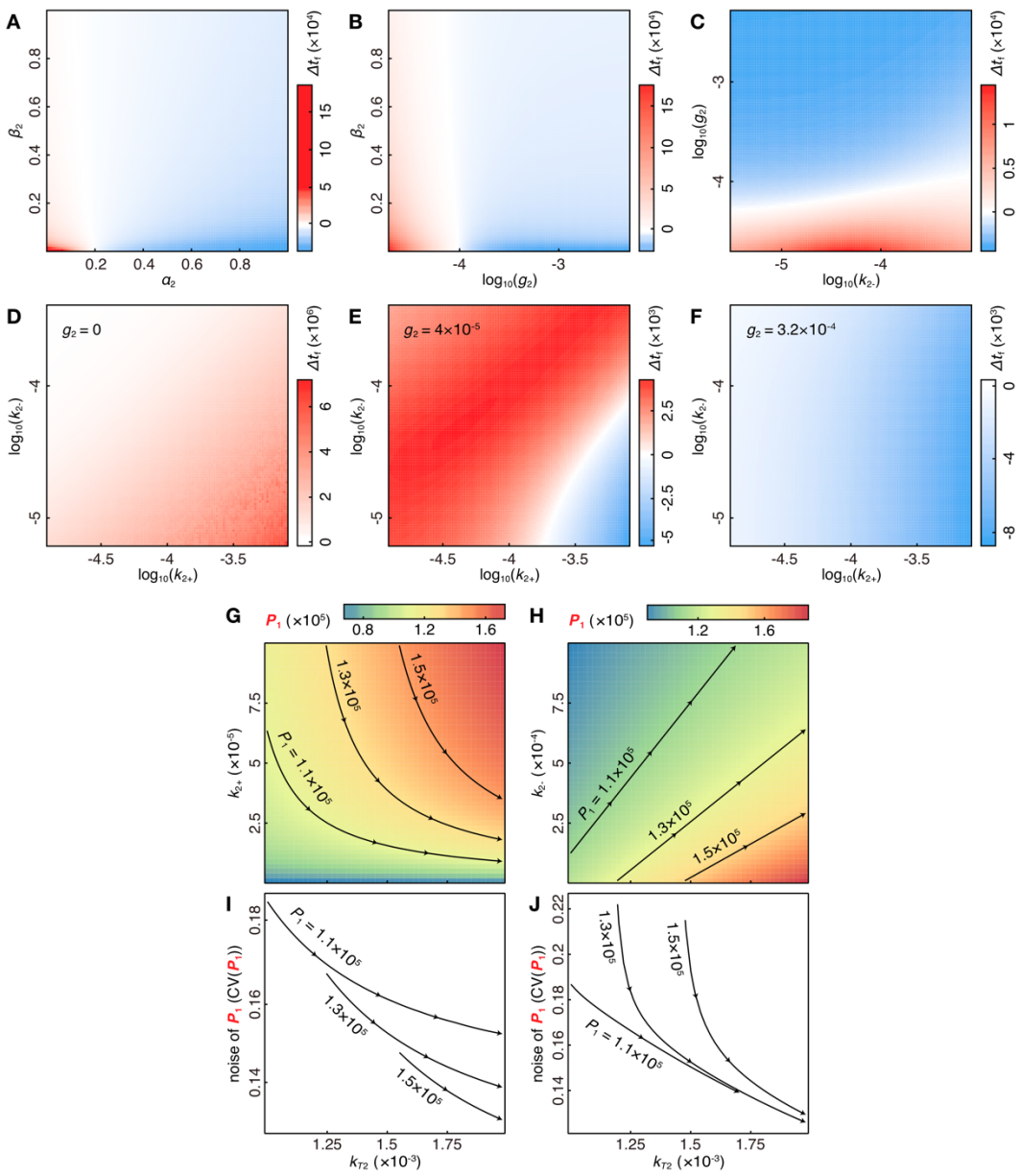

Figure S3 Dynamic properties of competition systems.

(*A-F*) Modifications of response time on the falling edge of *R*'s change under different kinetic parameters: (*A*) different α_2 and β_2; (*B*) different g_2 and β_2; (*C*) different k_{2-} and g_2; (*D-F*) different k_{2+}, k_{2-} and g_2 (values of g_2 are shown in figures).

(*G-J*) Abundant weak competitors can buffer target expression noise better. (*G-H*) P_1 level changing with T_2's production rate (k_{T2}) and T_2's association rate (k_{2+}) (*G*), or k_{T2} and T_2's dissociation rate (k_{2-}) (*H*). Black lines are T_1^F level isolines. (*I-J*) Target expression noise changes on the isolines in (*G*) and (*H*) respectively. Along the direction of the arrows, T_2's production increases and T_2's binding affinity decreases, bringing about lower expression noise.